Magnetic measurement with coils and wires

L. Walckiers
CERN, Geneva, Switzerland

Abstract
Accelerator magnets steer particle beams according to the field integrated along the trajectory over the magnet length. Purpose-wound coils measure these relevant parameters with high precision and complement efficiently point-like measurements performed with Hall plates or NMR probes. The rotating coil method gives a complete two-dimensional description of the magnetic field in a series of normal and skew multipoles. The more recent single stretched wire is a reference instrument to measure field integrals and to find the magnetic axis.

1 Introduction

The field of measurement of accelerator magnets has followed the requirements dictated by developments in accelerator technology. Synchrotron Light Sources require stringent magnetic axis alignment. The field quality of superconducting magnets for an accelerator like the Large Hadron Collider (LHC) has been measured to unprecedented precision, including the time and ramp rate dependent effects due to superconductor cables.

Measuring coils and more recently stretched wires are used extensively for accelerator magnets since they measure the parameters seen by particle beams: magnetic field components in the plane perpendicular to their trajectory and integrated over the length of the magnets. Coils and wires allow fast measurements with data already reduced to the requirements.

This field of physics has benefited from the development in electronic components. Fast acquisition voltmeters or recent 18-bit ADCs with sampling times in the range of microseconds increase the bandwidth and the precision of voltage integrated over time, the basis of this type of measurement.

Section 2 describes the classical method of coils flipped by half a turn inside dipole magnets or static coils in pulsed magnets. They are still in use to measure resistive dipoles having flat horizontal aperture and in particular for magnets having a small radius of curvature. In addition, the theory developed for these simple coils must be understood to avoid flaws with more sophisticated measurement methods. Section 3 introduces the concept of coil arrays to suppress the contribution from some harmonic components, a concept fundamental to the accurate use of the harmonic coil method.

Sections 4 to 7 group the Single Stretched Wire (SSW) based methods. They measure with high absolute precision the fundamental parameters of accelerator magnets. Section 4 introduces the equipment and demonstrates that the SSW gives an absolute value of the field integrated over the magnet length with a minimum of calibration concern. Section 5 details how to reference in all dimensions the position of the quadrupole magnet axis and field direction. Section 6 gives the most accurate method to quantify the integrated field gradient and address the issues related to wire deflection due to gravity and magnetic susceptibility. The vibrating wire method described in Section 7 is still subject to interesting developments in order to find the axis of individual magnets aligned on a girder. It is probably the only candidate method to measure small-aperture magnets under development for high-energy linear accelerators.

Sections 8 to 11 cover the harmonic or rotating coil method. This technique gives high resolution and measures in one coil revolution all relevant parameters of any accelerator magnet. Both theoretical and experimental developments allow one to confidently design sophisticated instruments measuring with high bandwidth and precision the full harmonic content of a magnet.

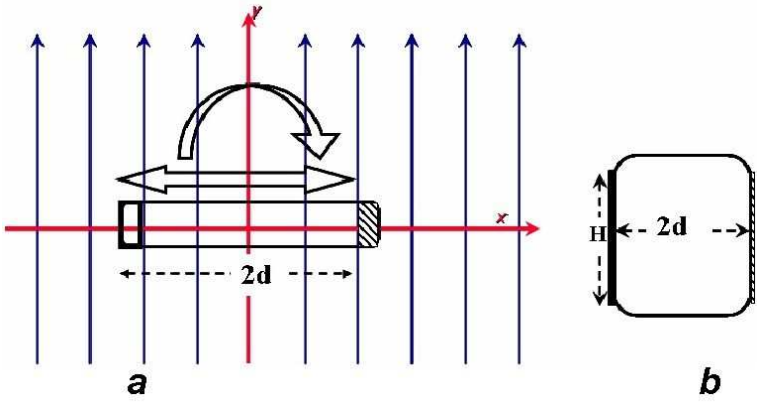

Fig. 1: (a) A simple coil, flipped in a dipole field to measure the central field, displaced laterally to measure the field quality. (b) Square coil with a single layer winding insensitive to the sextupole terms when $H = 2d$.

2 Coils to measure dipole magnets

The following section describes methods that measure only partially the 2D field along the axis of accelerator magnets. The rotating coil method (Section 8 and following) gives a complete measurement of any 2D field expressed in a formal way by a series of complex multipoles. It cannot, however, be used in the following cases which are relevant for most 'accelerator magnets' compared to storage rings:

- dipole magnets of small accelerators are bent,
- they mostly have wide horizontal apertures compared to the gap height,
- the rotating coil method does not (easily) measure pulsed fields, i.e., when $\Delta B/\Delta t$ cannot be neglected over one coil revolution period.

2.1 Flip coils for dipole magnet strength

The flux picked by the single-turn coil of width $2d$ sketched in Fig. 1(a) that is longer than the magnet of length L and that rotates by half a turn is

$$\Psi(\pi) - \Psi(0) = 2 \cdot \int_0^L \int_{-d}^{d} B_y(x) \cdot dx \cdot dl \ . \tag{1}$$

By assuming either a perfect dipole, i.e., $B_y(x, y)$ constant over the aperture or a coil of width $2d$ small compared to the field errors, i.e., the higher harmonics present in the magnet, the quantities relevant for the particle beam are deduced for the excitation current I in the magnet assumed to be constant during the time to flip the coil:

$$\text{Dipole strength} = \left[\int B_y \cdot dl\right](I) \qquad \text{in [T·m].} \tag{2}$$

$$\text{Transfer function} = \left[\int B_y \cdot dl\right](I)/I \qquad \text{in [T·m/A].} \tag{3}$$

The measuring coil has to be longer than the magnet. A rule of thumb says that the coil should extend outside both magnet ends by 2.5 times the aperture. To quantify the validity of this approximation, there is no other way than to perform a $B(z)$ scanning with a Hall plate or to make a full 3D calculation of the stray field in the magnet ends.

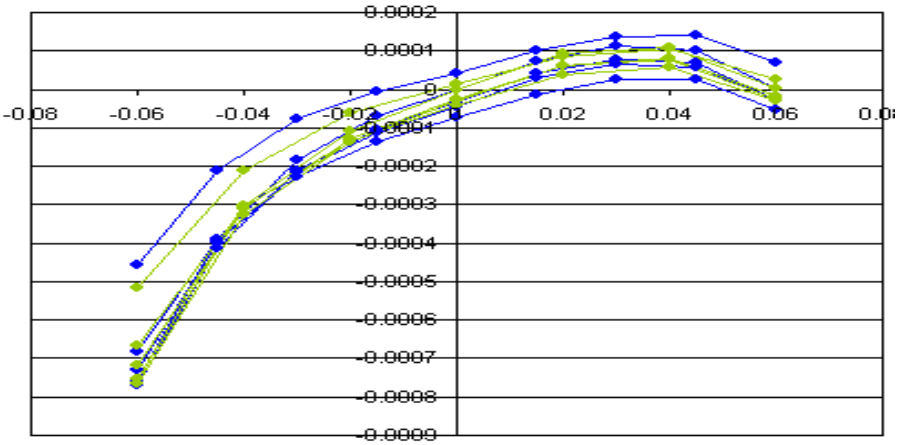

Fig. 2: $\Delta B_y(x)/\Delta x$ measured on 10 CNAO dipole magnets with the 11-coil fluxmeter

2.2 Coils displaced horizontally to measure the field quality

The first order imperfections to consider in a resistive magnet are the variation of the vertical field over the aperture width $\Delta B_y(x)$. The situation is more complex in superconducting magnets where a non-negligible horizontal field component $B_x(x)$ can be present in the horizontal mid-plane. The full 2D complex formalism has then to be applied to describe the field harmonics that can be measured by the rotating coil method covered from Section 8 onward. An horizontal displacement Δx of the coil of Fig. 1(a) leads per unit length along the magnet axis to

$$\frac{\Delta B_y(x)}{\Delta x} = \frac{\Psi(x+\Delta x) - \Psi(x)}{2d} \,. \tag{4}$$

Figure 2 gives the field quality in the horizontal symmetry plane of 10 dipole magnets for the CNAO facility (Section 3.3). These curves were measured, for efficiency reasons, in pulsed current mode by 11 different static coils rather than 10 horizontal displacements.

2.3 A real coil has finite dimensions for the winding

One way to increase the voltage amplitude at the coil terminals is to increase the width $2d$ therefore picking a vertical field non-constant over this width according to the field quality of the magnet. What is measured is no longer the field at the centre of the coil. The real part of Eq. (29) gives

$$B_y(x,y) = B_1 + B_2 \cdot x + B_3 \cdot (x^2 - y2) + \dots \,. \tag{5}$$

Integrating over the coil width going from $[x-d]$ to $[x+d]$ leads, with the hypothesis of a negligible winding height, to

$$\Psi(x) = B_1 \cdot 2d + B_2 \cdot 2dx + B_3 \cdot (6dx^2 + 2d^3) + \dots \,. \tag{6}$$

This equation indicates that a measurement with a half-turn flip is never sensitive to the even harmonics (quadrupole, octupole, etc.) as long as the axis of rotation is centred in the middle of the coil. On the other hand, the sextupole component enters in a dipole strength measurement:

$$\Psi(\pi, x=0) - \Psi(0, x=0) = 2.(B_1 \cdot 2d + B_3 \cdot 2d^3) + \dots \,. \tag{7}$$

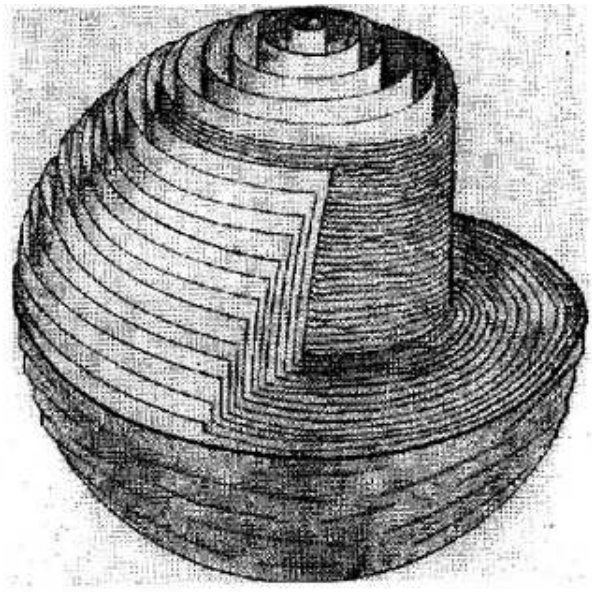

Fig. 3: A fluxball, composed of cylindrical windings, measures the field at the central point of the ball

All multipole terms enter with different and varying sensitivities when measuring the field quality by a displaced coil:

$$\Psi(x+\delta) - \Psi(x) = B_2 \cdot 2d\delta + B_3 \cdot 6d \cdot (2x\delta + \delta^2) + \dots . \tag{8}$$

Coils with several turns are used to further increase the sensitivity. The winding has then a non-zero cross-section. The coil of Fig. 1(b), with coil width equal to the winding height is easily calculated to have no sensitivity to the sextupole B_3 terms. The issue detailed by Eq. (7) for flip coil measurement is therefore limited to higher orders: starting with the decapole term present in the magnet.

This way of avoiding sensitivity to higher multipole terms was generalized in theory long ago with the fluxball [1]. This fluxball coil, as sketched in Fig. 3 seems difficult to manufacture but picks up a flux equal to the field at the centre of the ball and independent of the spatial harmonics present. A coil approximating this possibility of measuring the field central to a highly sensitive coil probe has been proposed in Ref. [2].

2.4 Static coils in pulsed fields

Most accelerator magnets have to be measured in fast current ramping conditions. The coil of Fig. 1(b), insensitive in that case to terms lower than the decapole, is an easy tool to use in fixed position in a field pulsed from 0 to nominal value. Modern integrators with large bandwidth and time resolution connected to such a coil can give the full $B_1(t)$ curve and measure saturation effects of the iron yoke. Hysteresis and eddy current effects can be separated by measurements at different ramp rates. One precaution deals with the remanent field of the magnet being measured, i.e., the field at zero current value. Three ways can be used to solve it:

- have a bipolar power supply to perform symmetric sweeps from negative to positive maximum current;
- demagnetize the magnet first, with either a bipolar supply or a supply with an inverter;
- measure the remanent field with a flip coil or Hall plates for instance, low accuracy is sufficient in most of the cases.

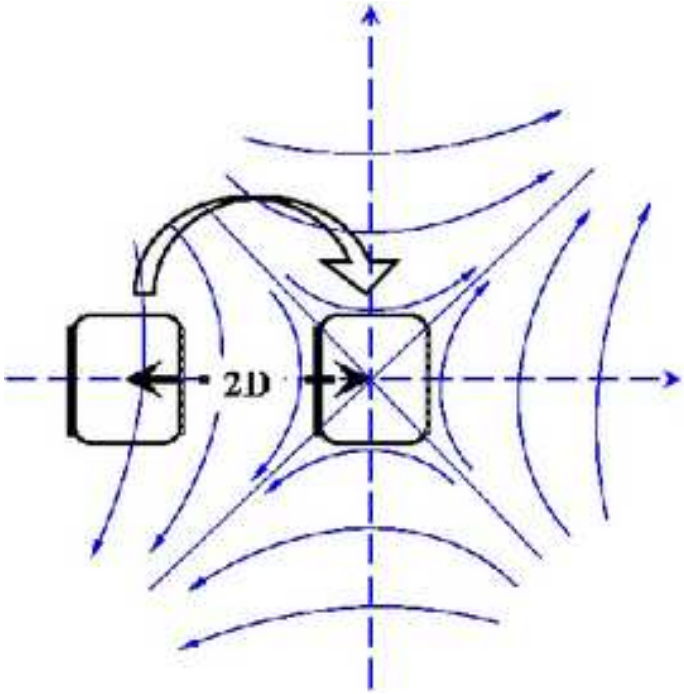

Fig. 4: Coil set to measure the gradient and field quality of a quadrupole magnet

3 Arrays of coils to measure quadrupoles or higher order multipoles

3.1 Two-coil array for quadrupole strength and field quality

The measurement of the strength of a quadrupole magnet could be done by the displaced coil method of Section 2.2. High accuracy requires high precision displacement of the coils and the measurement of the field quality, i.e., higher order multipoles, leads to a uselessly complex mathematical treatment. The array of two coils connected in electrical opposition and sketched in Fig. 4 is often used to give the quadrupole strength by flipping them about their symmetry axis. The coil array, i.e., the distance D, can be calibrated once in a known quadrupole. The field quality is deduced by displacing, along the x and y axis, the array in a quadrupole in the same way as the the single coil displacement to measure the field quality of a dipole magnet Section 2.2). Equation (9) is valid as long as the two coils have an equal effective surface.

$$B_1(x+D) - B_1(x-D) = 2 \cdot D \cdot G(x)\ . \tag{9}$$

The idea of using two coils connected in opposition in order to cancel the contribution of the dipole component is appreciably more effectively used with the rotating coil method (Sections 9.3 and 9.5). In that case, the compensation scheme suppresses the main harmonic of the magnet. It is therefore much more powerful for accurate field quality measurements. The rotating coil equipment is more complex to manufacture but is preferred for quadrupole magnets that are straight and have a circular aspect ratio. The present method is, however, mentioned as useful for combined-function magnets and pulsed magnet measurements.

3.2 The Morgan coil for pulsed magnets

G. H. Morgan [3] proposed a complex coil array that can measure any multipole magnet, or magnet component, in pulsed mode, i.e., with static coil array. Identical coils are located around a cylinder frame with the symmetry to be measured. The number of coils is equal to the multipole order to be measured: three coils for a sextupole, etc.

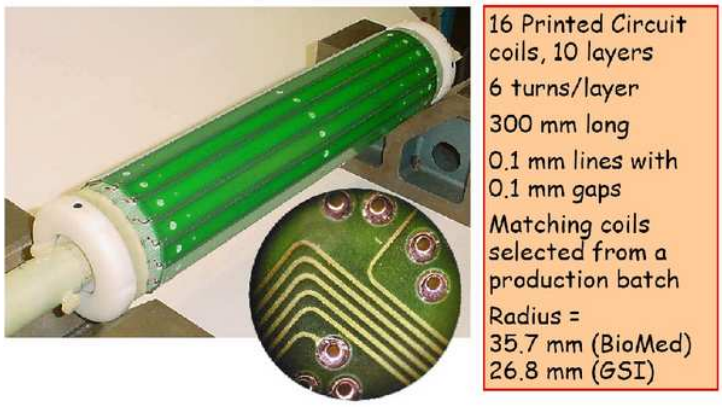

Fig. 5: Measuring shaft with 16 individual coils made with printed circuit technology. A large number of harmonics can be measured in pulsed mode by using various connection schemes (courtesy of A. Jain, BNL).

.

Fig. 6: (a) The CNAO fluxmeter with 11 curved coils, (b) inserted in one of the CNAO dipole magnets

Figure 5 details an array of coils able to measure a large number of harmonics by different connection schemes to put in series the individual coils. Small discrepancies between the individual coils can be eliminated by turning the coil frame at different angular positions. One should not forget that a coil scheme sensitive to a multipole of order n is as well sensitive to order $n \cdot (2m + 1)$. Reference [4] describes the full theory of this technique.

3.3 A dedicated coil array to measure curved dipoles in pulsed mode: the CNAO fluxmeter

A dedicated array of 11 curved coils has been assembled to measure the CNAO dipole magnets [5]. These 1.5 T dipoles have a bending of $22.5°$ and operate with a field rise time of 2 seconds. Eddy current effects present in particular in the ends of the magnet yoke have to be taken into account for both the field integral as a function of current and the field quality over the 130 mm useful aperture.

Figure 6(a) shows the 11 coils fixed on the frame that can be entered from a zero field region into one magnet end to measure the remanent field, or measure in static position during the field ramp [Fig. 6(b)]. A cross-calibration 12th coil can be mounted on top of each individual coil of the fluxmeter. This cross-calibration gave correction factors to equalize the effective width of the 11 coils within 10^{-4} relative accuracy.

Note that all correction factors described in Section 2.3 have to be applied to calculate the field errors in terms of multipoles. Figure 2 gives the vertical field component in the horizontal symmetry plane of 10 CNAO dipole magnets measured with this fluxmeter, taking into account these systematic errors.

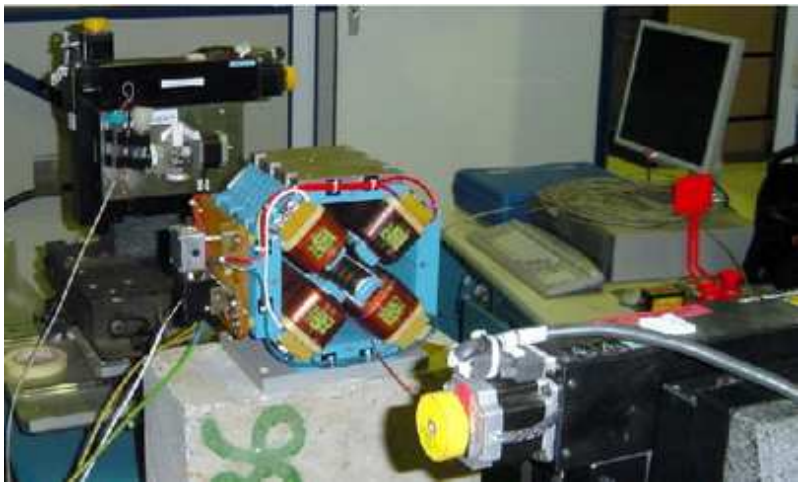

Fig. 7: The SSW equipment installed to measure a quadrupole magnet. The wire is displaced in the quadrupole aperture by 2D high-precision stages on both sides.

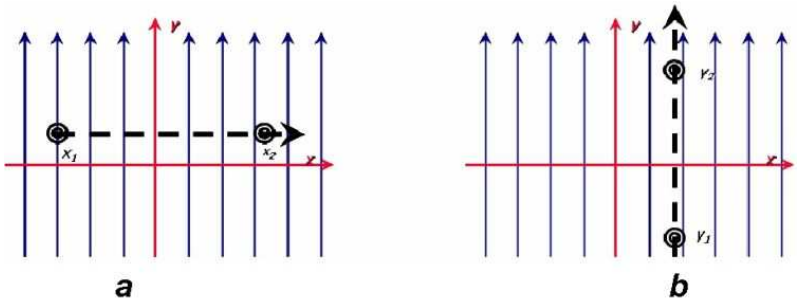

Fig. 8: (a) The single stretched wire displaced horizontally to measure the field integrated over the dipole length. (b) A vertical displacement gives zero signal if displacement and field direction are parallel.

4 The single stretched wire technique with a dipole magnet

Particle beams are sensitive to field integrated along their trajectory. The SSW (Single Stretched Wire) method consists of a high tensile conducting wire moved inside the magnet aperture by precision displacement tables. CuBe wires 0.1 mm thick are commonly used. The stages at both sides are assumed to move by precisely the same amount. The return wire is kept fixed, as much as possible in a field-free region. The flux lines crossed during this displacement, $\Psi(x_1, x_2)$, and measured by a voltage integrator give the field integrated over the displacement, $d = x_2 - x_1$, and over the SSW length, $L_{\rm w}$. Figure 7 shows the system developed by FNAL [6] and mounted to measure a quadrupole magnet. When measuring a perfect dipole ($B_y = Cst$, $B_x = 0$) as in Fig. 8(a) the integrator gives

$$\Psi(x_1, x_2) = \int_0^L \int_{x_1}^{x_2} B_y(x, l) \cdot dx \cdot dl = d \cdot \int B \cdot dl \ . \tag{10}$$

The measurement accuracy of the dipole strength is linked to the calibration of the integrator gain $(10^{-4} - 10^{-5})$ and to the precision of the mechanical displacement. Commercially available stages reach an accuracy better than $10^{-4} = 1$ µm/10 mm. This method was cross-checked 30 years ago against NMR mapping and gave agreement within few 10^{-5}.

Similarly, a vertical displacement in a dipole aligned vertically gives a zero flux variation [see Fig. 8(b)]. It is the simplest and most accurate method of finding the field direction of a dipole: accuracies of 0.1 mrad are commonly reached.

This method is simple and efficient to measure the first integral of wigglers and undulators. This first integral value, given by Eq. (10), corresponds to the angular deflection of the beam and is tuned to be zero in the relevant cross-section of the magnet. It has been complemented by the pulsed wire technique to measure and tune the second field integral value [7, 8]. Travelling Hall plate based measurements are nowadays preferred since in addition they give more details on the regularity of the undulator periods.

5 Align a quadrupole with the single stretched wire

The single stretched wire technique is relevant to finding the axis, main field direction, and longitudinal position of a quadrupole magnet [6]. These three alignment steps will be treated separately so as to be easily understood. An automated acquisition system is better for iterating changes in the reference position of the wire for both stages according to full measurement cycles until an accurate coincidence between wire and magnet axes is reached.

A pure quadrupolar field is defined by

$$B_y = G \cdot x \quad , \quad B_x = G \cdot y \; . \tag{11}$$

The magnetic axis is defined by the line where

$$B_x = B_y = 0 \; . \tag{12}$$

The main field direction is defined by the symmetry planes:

- $B_x = 0$ in the horizontal symmetry plane,
- $B_y = 0$ in the vertical symmetry plane.

Moving a SSW vertically from position y_1 to position y_2 [Fig. 9(a)] gives the measured flux of Eq. (13), i.e., a parabolic dependence. The effective length L_{eff} hides the integral over the magnet length.

$$\Psi(y_1, y_2) = \int_0^L \int_{y_1}^{y_2} G \cdot y \cdot dy \cdot dl = L_{\text{eff}} \cdot \frac{G}{2} \cdot (y_2^2 - y_1^2) \; . \tag{13}$$

A further correction must be applied to take into account the wire sagitta that could reach millimetres for a 10 to 15 m long distance between the stages. The system of Fig. 7 incorporates a driver to make the measurement with different wire tensions (Fig. 11). The measurement data are extrapolated to infinite tension. This will be detailed in Section 6.1 since this error source is more detrimental for the measurement of the strength of a quadrupole. To obtain accuracy in the result requires therefore time, even with fully automated equipment and procedures, since loops at different tensions are internal to iteration to align the wire coordinate system to the magnet axis. An accurate measurement of the gradient can only take place after a full alignment procedure.

5.1 Align the quadrupole axis and field direction

Equation (13) tells us that two measurements are needed to find y_c, minimum of the parabola giving the horizontal plane where the axis is located. The method in use is to measure in an iterative way the fluxes over two equal intervals then displace the central point of the measurement y_c until the following condition is reached:

$$\Psi(y_c, y_c + d) = \Psi(y_c, y_c - d) \; , \tag{14}$$

$$(y_c + d)^2 - y_c^2 = (y_c - d)^2 - y_c^2 \; . \tag{15}$$

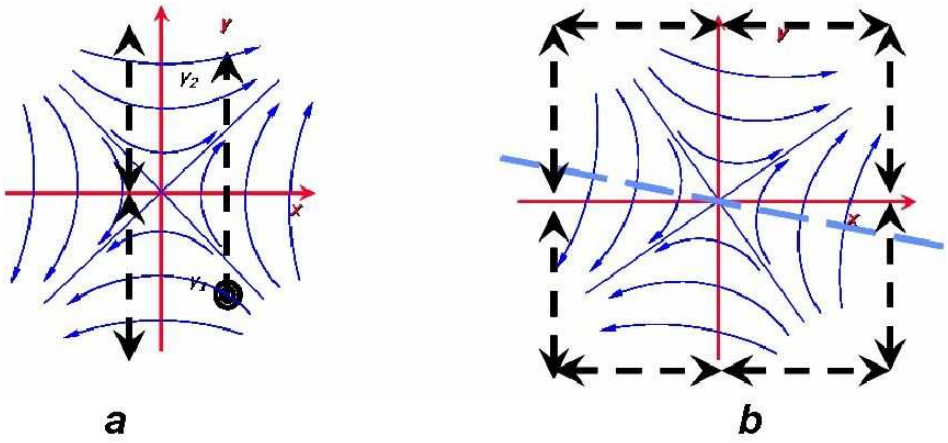

Fig. 9: (a) The single stretched wire displaced vertically in a quadrupole. Two measurements are needed to find the minimum of the parabolic dependency, i.e., the horizontal symmetry plane. (b) The axis and field direction (i.e., tilt of the quadrupole field) are found with eight measurements.

The point where $B_x = 0$ is found for a given vertical line. The main field direction is found by displacing this movement line along x, and the vertical symmetry plane is found by equivalent horizontal displacements. A full measurement is done by the eight displacements of the external square of Fig. 9(b) and repeated until the SSW coordinate system coincides with the quadrupole axis. It is obviously important that the two stages move parallel to each other.

5.2 Stretched wire non-parallel to the quadrupole axis

Figure 10(a) sketches, for the vertical direction, how to tune the parallelism between the SSW and magnet axes. A displacement of one stage going from an angle α_1 to α_2 with respect to the magnet axis gives a flux:

$$\Psi(\alpha_1, \alpha_2) = \int_{\alpha_1}^{\alpha_2} \int_{L_1}^{L_2} G \cdot \alpha \cdot l \cdot dl \cdot d\alpha \;\; = \;\; G \cdot \frac{\alpha_2^2 - \alpha_1^2}{2} \cdot \frac{L_2^2 - L_1^2}{2} \; . \tag{16}$$

The effective length of the magnet $(L_2 - L_1)$ should be known, and the middle of the magnet is supposed to coincide with the middle of the wire. This is, however, of minor importance since this method, similarly to the one of Section 5.1, implies a series of two symmetric displacements iterated until the parallelism is found, i.e., until they give equal flux values.

5.3 Measure the longitudinal location of the magnet

Once the magnet is fully centred and the axis is parallel to the wire reference position, anti-parallel movements of the wire give the longitudinal position d of the magnet with respect to the middle of the wire length L_{w} [Fig. 10(b)]. The angular movement α has to be symmetric with respect to the magnet axis. The flux for such angular movement is given by

$$\Psi(\alpha_1, \alpha_2) = \int_{\alpha_1}^{\alpha_2} \int_{L_1}^{L_2} G \cdot x(\alpha \cdot l) \cdot dl \cdot d\alpha = G \cdot \frac{\alpha_2^2 - \alpha_1^2}{2} \cdot d \cdot L_{\mathrm{eff}} \; , \tag{17}$$

with

$$x = \left(l - \frac{L_{\mathrm{w}}}{2} \right) \cdot \alpha \; , \quad L_1 = \frac{L_{\mathrm{w}} - L_{\mathrm{eff}}}{2} + d \; , \quad L_2 = \frac{L_{\mathrm{w}} + L_{\mathrm{eff}}}{2} + d \; .$$

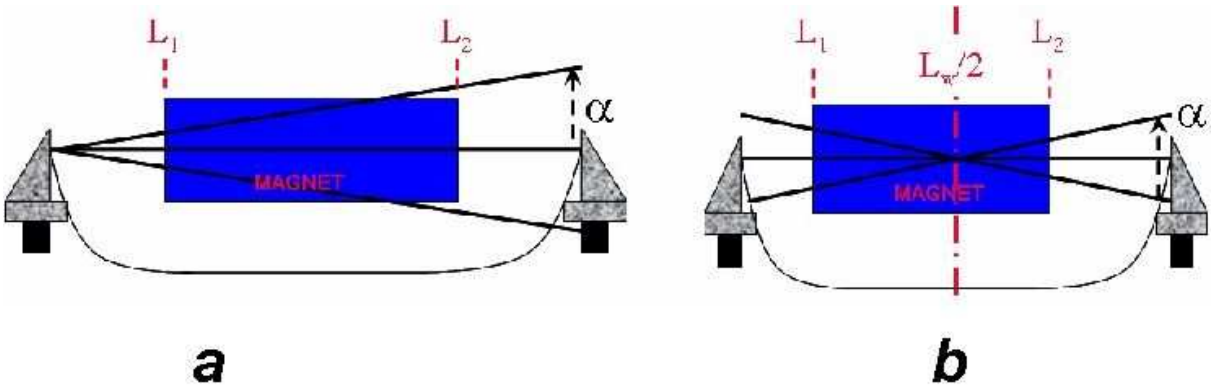

Fig. 10: (a) Two angular displacements give the same result if done symmetrically with respect to the quadrupole axis, i.e., when this axis and the reference line of the SSW coincide. (b) The same angular displacements with the fixed point at the middle of the SSW length give the distance between this SSW middle and the middle of the magnet length.

5.4 Automatic alignment of the SSW reference system to the quadrupole axis in all directions

The system has to be designed to automatically align the SSW with respect to a quadrupole according to these various principles put together. The SSW reference system is aligned iteratively, by one compound measurement with eight co-parallel and eight counter-parallel displacements according to Fig. 9(b), followed by modifications of the SSW reference system. This alignment campaign is tedious since each of these 16 data sets has to be done with different tensions of the wire to extrapolate the results to infinite tension, as detailed in Section 6.1. The longitudinal location is calculated with the last measurement data. The precision obtained with the FNAL equipment for wires up to 16 m long is remarkable: about 0.1 mm for the axis at both magnet ends and 0.03 mm for the integral, 5 mm for the longitudinal position.

6 Measure the integrated strength of a quadrupole with the SSW

The difficulties encountered when measuring a quadrupole strength are that the wire has a natural deflection in the millimetre range if the wire or magnet length reaches several metres. In addition, it is difficult to find CuBe wire that has zero magnetic susceptibility. Unfortunately the industrial standards describing this type of material rarely include the impurity content of non-zero susceptibility. Several batches purchased from the same manufacturer could have appreciably different magnetization and the only way to sort the best batch is to test with a permanent magnet. In conclusion the wire deflection depends on the position in the quadrupole cross-section, in both amplitude and direction. The accuracy is also limited by the high order multipoles present in the magnet that perturb the value of $G \cdot L_{\text{eff}}$ obtained from Eqs. (13)–(15). The only way to estimate accurately that error source is to perform a full measurement of the multipole content for instance with the rotating coil system (Section 8). These perturbations grow with the distance from the magnet axis, and a detailed estimation is needed to either limit the range of the displacement allowed or to include relevant correction factors in the data analysis. In practice, the estimation of the quadrupole strength is obtained from the last set of data measured once the SSW reference system is fully aligned with the quadrupole axis (Section 5).

6.1 Extrapolate the results to infinite tension of the wire

The sagitta due to gravity can easily amount to millimetres with a CuBe wire at maximum tension. The wire tension is measured by the vibration frequency f to get enough precision. This vibration can be induced by the stage motors giving a horizontal or vertical kick and is sensed via the voltage across the wire since it oscillates in a magnetic field. An extrapolation to infinite tension is usually done by looking

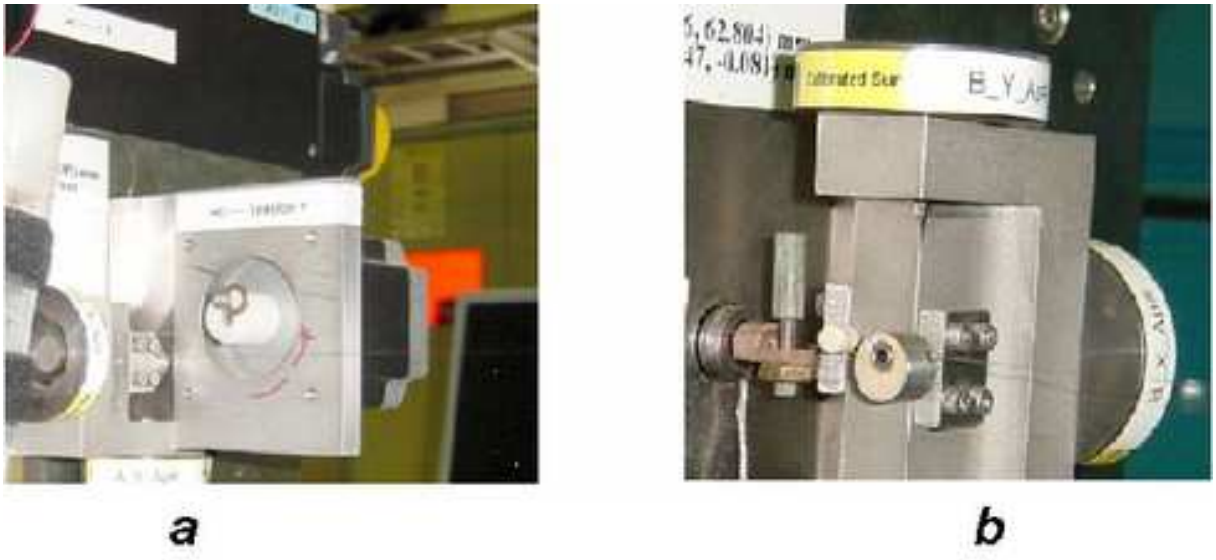

Fig. 11: (a) Stepping motor to adjust the wire tension in order to extrapolate the measurement to infinite tension. (b) Tension gauge used to drive the stepping motor at the expected tension.

at the curve of the integrated gradient measured as a function of the measured $1/f^2$, i.e., proportional to the wire tension according to the following relations:

$$\text{sag} = \frac{W \cdot g}{8T} L_{\text{w}}^2 \tag{18}$$

$$f = \frac{1}{2L_{\text{w}}} \sqrt{\frac{T}{W}} \tag{19}$$

with W the weight of the wire per unit length, g the gravity constant, and T the wire tension.

Figure 11(a) shows the remotely controlled actuator to change the wire tension. Figure 11(b) shows a tension gauge used to control the adjustment of the tension in particular to avoid breaking the wire.

6.2 Measure the gradient with horizontal displacements of the wire

Figure 12 shows the curves of the transfer function obtained at different currents into an LHC quadrupole magnet [9] for a given type of CuBe stretched wire. Three observations can be made about this measurement campaign summarized in Table 1:

- the slope of the measured gradient depends, as expected, on the frequency but also on the square of the gradient, i.e., the current in the quadrupole magnet;
- gradient values measured by vertical displacements were found to be systematically higher than with horizontal displacements;
- this dependence on the gradient is different according to the batch of CuBe wire used, and this finding correlates with the wire being paramagnetic or diamagnetic as sensed by a permanent magnet.

A detailed analysis proved that the $1/f^2$ dependence was linear for horizontal displacements but not for vertical displacements. This is explained by looking at the dependence of the magnetic forces in both cases. The force variation due to the field gradient is horizontal for an horizontal displacement:

$$F_x \propto G^2 \cdot (x_{\text{step}})^2 \,, \tag{20}$$

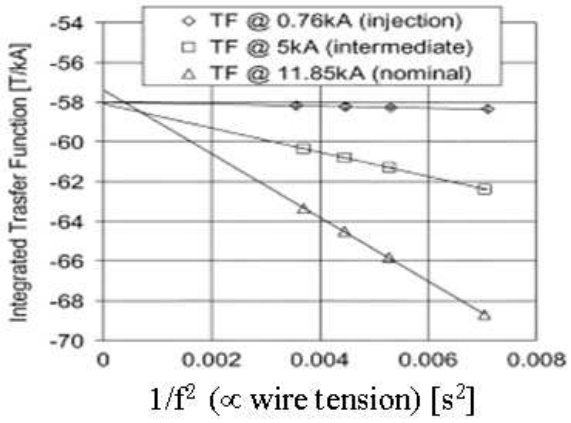

Fig. 12: Measured gradient, integrated over the quadrupole length, divided by the current as a function of the wire tension measured by the vibration frequency

Table 1: Slopes of measured quadrupole strength, as a function of inverse squared vibrating frequency, for different types of wire, in [T/s^2].

Wire No.	0.76 kA	5 kA	11.5 kA	χ
1	30.4	2000	9500	paramagnetic
2	6.1	500	5000	paramagnetic
3	2.3	50	474	diamagnetic
4	–	–	380	diamagnetic

but has a parabolic dependence with vertical displacements

$$F_y \propto G^2 \cdot (y_{\text{step}} + \text{sag})^2 \, . \tag{21}$$

The gradient obtained with vertical displacements should therefore be calculated with a fit to a parabolic law, so is less stable than for the horizontal displacements. It is therefore better to choose the result obtained with the horizontal displacements.

Relative discrepancies of $2 \cdot 10^{-4}$ for the measured gradient were obtained between measurement with vertical and horizontal displacements, giving an estimate of the accuracy that can be obtained with this method.

7 The vibrating wire technique

Mechanical oscillations of the stretched wire can be induced by the Lorentz force created by AC current flowing into the wire going through the static field of the measured magnet. This technique, proposed by A. Temnykh, has sub-micrometre sensitivity to sense a quadrupole axis. It can be used to measure separately the axis of several magnets aligned on a girder and has been extended to find sextupole axes.

Reference [10] details the resolution of the differential equation to solve for standing wave solutions:

$$W\frac{\partial x^2}{\partial t^2} = T\frac{\partial x^2}{\partial z^2} - \gamma\frac{\partial x}{\partial t} + I(t)B(z) \tag{22}$$

with $x(0,t) = x(L_{\text{w}},t) = 0$ the boundary conditions, W the weight of the wire per unit length, T the wire tension, γ the damping coefficient, $I(t) = I_0 \cdot e^{i\omega t}$ the driving AC current, and $B(z)$ the transverse magnetic field.

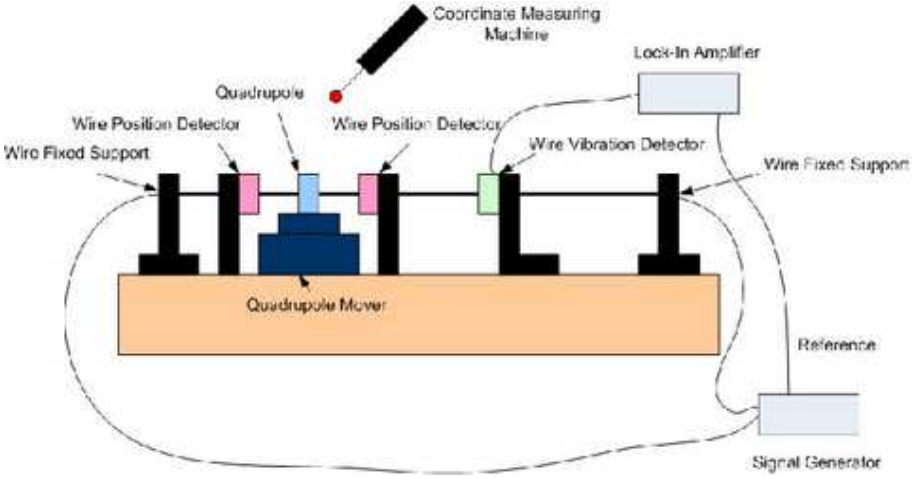

Fig. 13: Overview of the vibrating wire equipment measuring the magnetic axis in a quadrupole. The wire vibration detector and the quadrupole are longitudinally located to have maximum signal with the second harmonic of the natural oscillation frequency (courtesy of Z. Wolf, SLAC).

The solution is a sum of standing waves of amplitudes x_n that can be measured. From there the B_n coefficients of a sinus wave expansion of $B(z)$ are estimated

$$x(z,t) = \sum x_n \sin\left(\frac{\pi n z}{L_\mathrm{w}}\right) e^{i\omega t} \,, \tag{23}$$

with

$$x_n = \frac{I_0}{W} \cdot \frac{1}{\omega^2 - \omega_n^2 - i\gamma\omega} \cdot B_n \,,$$
$$\omega_n = \frac{\pi n}{L_\mathrm{w}} \sqrt{\frac{T}{W}} \,.$$

$B(z)$ can be reconstructed knowing the series of B_n:

$$B(z) = \sum B_n \sin\left(\frac{\pi n z}{L_\mathrm{w} w}\right) \,. \tag{24}$$

In practice, the AC current is tuned to the natural oscillation frequency f_nat of the wire or one of its harmonics $m \cdot f_\mathrm{nat}$. The amplitudes of these oscillations are measured by inexpensive photo interrupters. The wire motion in the vertical, respectively horizontal, plane is caused by the Lorentz forces between the wire current and the horizontal, respectively vertical, magnetic field. Therefore two wire vibration detectors are mounted orthogonal to each other.

A procedure to centre one quadrupole is straightforward. The wire oscillation detectors can be located in a longitudinal position where the amplitude is large for the vibration harmonic considered. That is why it is separated from the position detectors in Fig. 13 that gives an overview of the equipment [11]. Since the Lorentz force is zero if the wire is aligned with the quadrupole axis, the magnet or the wire can be moved until vanishing oscillations are seen in both planes. Some coupling between the measured oscillations in both directions could exist due to imperfect orthogonality between the detectors. It has to be measured and taken into account to achieve high accuracy (Fig. 14). These measurements obtained by wire motion controlled by piezo-electric actuators demonstrate the sub-micron resolution [12].

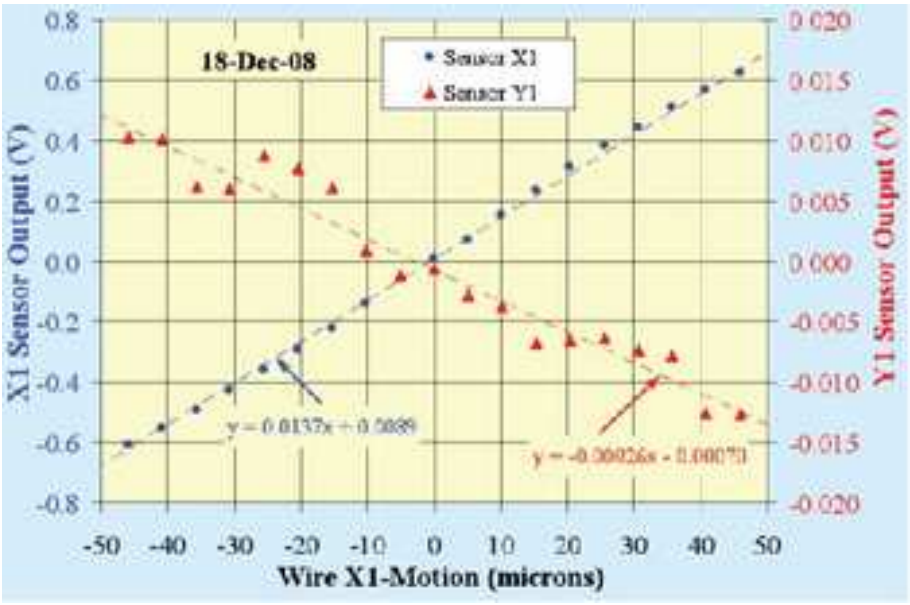

Fig. 14: Amplitudes measured by the x and y photocouplers for small displacements of the vibrating wire around the quadrupole axis in the x direction (courtesy of A. Jain, BNL)

8 Description of the harmonic coil method

The harmonic coil method was developed with early analog integrators forcing the measuring coil to rotate stepwise between consecutive angular positions [13]. Fast angular encoders and purpose-developed voltage integrators with zero dead time between the angular positions are the basis of today's systems acquiring several hundred points per turn with a rotation rate as high as 10 turns per second. It is the best method for measuring higher order multipoles within a well-established theoretical frame, in particular of superconducting and quadrupole magnets having circular apertures. Progress in data acquisition equipment and data analysis tools alleviates the complexity of the formalism applied to the amount of data to treat, so that fully automated instruments and data analysis processes have been developed for measurements of series of magnets with high confidence in the final results.

8.1 Flux enclosed by a simple rotating coil

A perfect dipole magnet gives a constant vertical field everywhere in the useful aperture. The flux enclosed by the simple coil described in Fig. 15 will be, considering an infinitely thin winding,

$$\Psi(\theta) = N_{\mathrm{t}} \cdot L \cdot \int_{R_1}^{R_2} B_1 \cdot \cos\theta \cdot dR \,. \tag{25}$$

N_{t} and L are respectively the number of turns and length of the measuring coil. The coil is supposed to be shorter than the magnet. The coil's effective surface can be calibrated independently and is given by

$$\Sigma_{\mathrm{coil}} = N_{\mathrm{t}} \cdot L \cdot \int_{R_1}^{R_2} dR = N_{\mathrm{t}} \cdot L \cdot (R_2 - R_1) \,. \tag{26}$$

The use of a voltage integrator connected to the measuring coil makes it possible to eliminate the time coordinate in the induction law of Faraday. The voltage integrator read as a function of the angle gives the flux directly from the zero angle where it is reset. The constant of integration is irrelevant for this method.

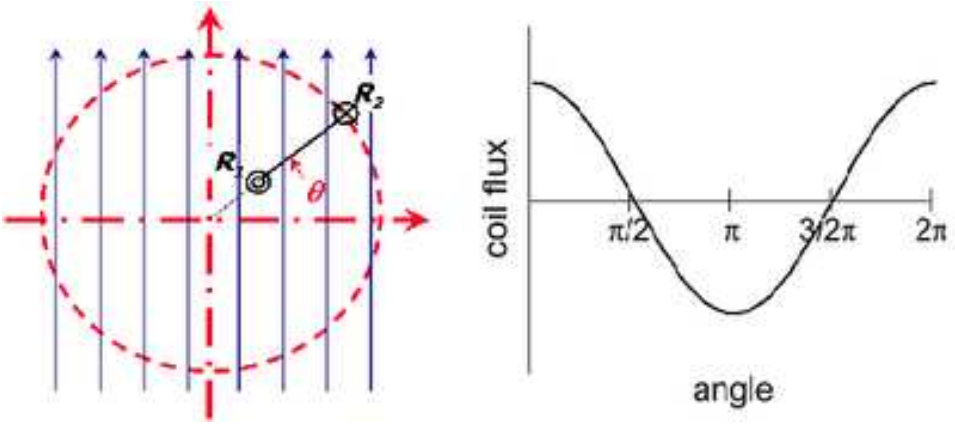

Fig. 15: 2D representation of the flux seen by a simple coil rotating in a dipole field

The units of Eq. (25) are

$$\Psi = \text{volt} \cdot \text{sec} = \text{tesla} \cdot \text{m}^2 = \text{weber} \; . \tag{27}$$

It is important to realize that the harmonic coil method does not make use of the voltage integrated over a given time, but rather over a given angular interval. The advantage of using a voltage integrator that can be externally triggered is that it eliminates to the first order the problem of a constant speed of rotation. A real system in fact measures differences of fluxes between two incremental angular positions. The angular encoder mounted on one coil end is a fundamental piece of equipment, as described in Section 9.2. The integrator is triggered by this encoder and collects incremental fluxes $\delta\Psi_k$, and the left part of Eq. (25) becomes

$$\Psi(\theta_i) - \Psi(\theta_0) = \sum_{k=1}^{i} \delta\Psi_k \; , \tag{28}$$

with

$$\delta\Psi_k = \Psi(\theta_k) - \Psi(\theta_{k-1}) \; .$$

8.2 Formalism for multipoles measured by rotating coils

The power of the harmonic coil method is its ability to measure any type of 2D magnetic field. It can be demonstrated [14] that a rotating coil measures the 2D field integrated over its length as long as the field component parallel to the rotation axis is zero on the two coil ends. The complex equation to best describe this 2D field is

$$B(x + i \cdot y) = B_y(z) + i \cdot B_x(z) = \sum_{n=1}^{\infty} C_n \cdot \left(\frac{z}{R_\text{r}}\right)^{n-1} \; . \tag{29}$$

The components $C_n = B_n + iA_n$ are the normal and skew multipoles of the field. By definition for accelerator magnets, the normal components indicate a vertical field in the horizontal plane whilst the 'skew' terms apply for an horizontal field. The C_n are in tesla at the reference radius R_r. Figure 16 shows the field lines for normal and skew dipoles (C_1) and quadrupoles (C_2).

The field quality is usually described as errors relative to the main field component B_M ($M = 1$ for a dipole, $M = 2$ for a quadrupole) at the reference radius R_r. These errors are called 'units' and are given by

$$c_n = b_n + i \cdot a_n = 10^4 \frac{C_n}{B_M} \; . \tag{30}$$

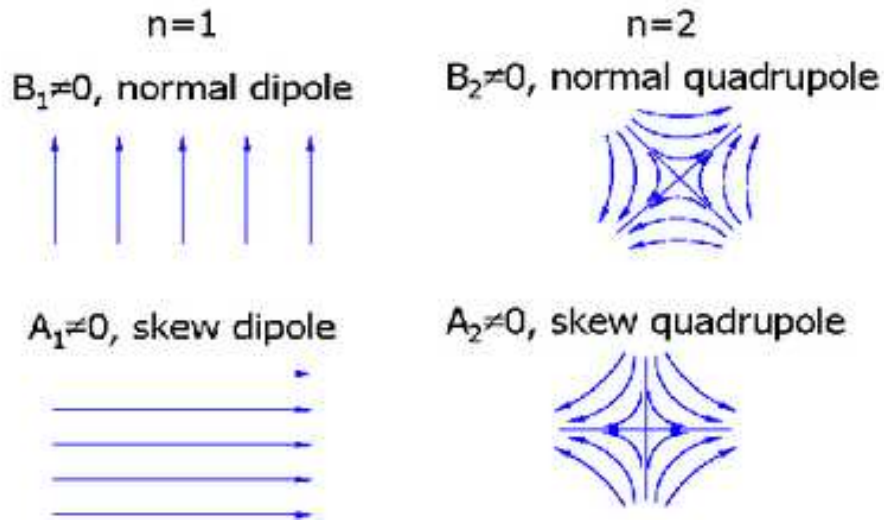

Fig. 16: Field lines of normal and skew dipole and quadrupole magnets

The reference radius R_{r} is an important concept for accelerator magnets having apertures much smaller than one metre. R_{r} corresponds in practice to

- the useful aperture for the beam,
- 2/3 of the yoke aperture in resistive magnets,
- 2/3 of the coil aperture in superconducting magnets,
- the radius where the multipoles relative to the main field, the c_n in Eq. (30), have the same order of magnitude in a real magnet.

It is important to carefully choose this reference radius at the beginning of a project. It will intervene in the discussions between all actors involved: beam optic physicists, magnet designers, measurement crew, and data analysis teams.

The voltage integrated over a simple rotating coil described in Fig. 15 and rotating in any 2D field will therefore be

$$\Psi(z) = N_{\mathrm{t}} \cdot L \cdot \mathrm{Re} \int_{R_1}^{R_2} B(z) \cdot \mathrm{d}z \; . \tag{31}$$

Since the coil rotates

$$z = x + i \cdot y = R \cdot e^{i\theta(t)} \; . \tag{32}$$

And by applying Eq. (29) and integrating it over $\mathrm{d}R$

$$\Psi(\theta = \omega \cdot t) = \mathrm{Re} \left(\sum_{n=1}^{\infty} N_{\mathrm{t}} \cdot L \cdot \frac{R_2^n - R_1^n}{n \cdot R_{\mathrm{r}}^{n-1}} \cdot C_n \cdot e^{in\theta} \right) \; . \tag{33}$$

This allows a formal separation between what belongs to

- the measured field components C_n,
- the time dependence of the signal $e^{\mathrm{i}n\theta(t)}$,
- the coil sensitivity factor K_n defined as

$$K_n = N_{\mathrm{t}} \cdot L \cdot \frac{R_2^n - R_1^n}{n \cdot R_{\mathrm{r}}^{n-1}} \; . \tag{34}$$

The K_n are calculated once for each measuring coil used. As will be detailed in Section 10 they can be complex numbers in the case of tangential coils, or coils not perfectly aligned radially. These calculations are substantial if the windings can no longer be considered point-like. Their values can be improved by individual calibrations [15].

The power of the harmonic method is that the multipoles of the field are directly given by the Fourier analysis coefficients Ψ_n of the integrated voltage over a coil turn $\Psi(\theta)$:

$$\Psi_n = K_n \cdot C_n = K_n \cdot (B_n + iA_n) \; . \tag{35}$$

8.3 Centre the measurement results by measuring the field axis and direction

The harmonic method measures with high accuracy the direction of the main field component with respect to the measuring coil direction. It gives as well the axis of a quadrupole or sextupole magnet with respect to the rotation axis of the measuring coil. These measurements are fundamental for accelerator magnets since the beam closed orbit is defined by the residual tilt of the dipole magnets and the quadrupole misalignments. This property is also useful to align the set of measured multipoles in the symmetry axis of the magnet. This was required, for instance, for the system described in Fig. 17 where the 12 intermediate bearings of the 15 m long measuring shafts are poorly centred with respect to the superconducting magnet. Simple equations given below formally change the reference axis system of the multipole set.

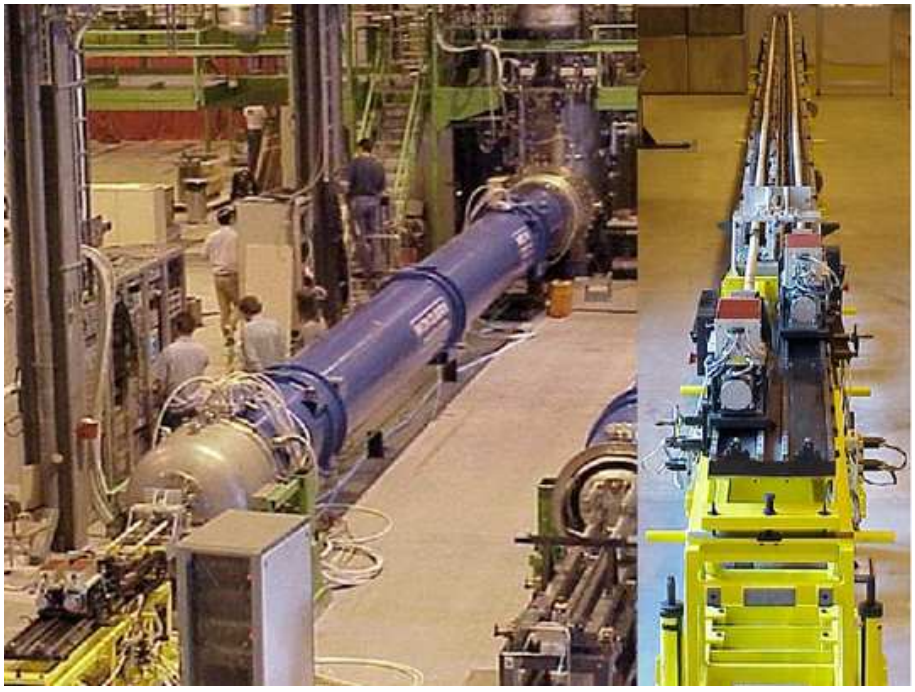

Fig. 17: LHC superconducting magnets measured with a 15 m long shaft. The 'Twin Rotating Unit' at the bottom of both pictures holds the motors and encoders.

8.3.1 Find the main field direction

The harmonic coil method gives the field description, the C_n in Eq. (35), in the reference frame defined by the measuring coil when at θ = 0, usually given by the reference angle of the encoder. The main field direction corresponds to a zero main skew term (A_1 = 0 for a dipole magnet). This main field direction often does not correspond with enough accuracy to the magnet mechanical symmetry plane, hence the

usefulness of this measurement. In addition, both the magnet and measuring system may not be aligned with gravity, used as an external reference. Three frames are considered:

- θ_m : zero of the encoder, reference for the Fourier analysis;
- θ_g : gravity, magnet fiducials when aligned;
- θ_f : field direction of the magnet (A_1 = 0 for a dipole magnet).

To rotate the multipole coefficients from one frame to another is straightforward from Eq. (33). Assuming respectively θ_m and θ_f the angles of the measurement frame and the magnet symmetry plane with respect to gravity give:

$$z_f = z_m \cdot e^{i(\theta_m - \theta_f)} \,, \tag{36}$$

$$C_{m,n} = C_{f,n} \cdot e^{in(\theta_m - \theta_f)} \,. \tag{37}$$

The accuracy of finding the field direction in the coil reference frame is high: typically better than 0.1 mrad. The difficulty is to find the coil reference direction with respect to an external reference. The coil average winding position is commonly misaligned by a few mrad with respect to the coil frame. In addition, extreme care is needed to have a perfect alignment with respect to the encoder reference angle. An easy calibration is possible by turning end to end either the magnet to be measured or the encoder plus coil set. It was possible, on account of the size of the magnets to be measured, to design the bench shown in Fig. 18 for this easy calibration.

8.3.2 Coil rotation axis different from the magnet symmetry axis

Similarly, the measuring coil does not necessarily rotate about the magnet axis. The reference frame, where $z_c = 0$, of the magnet axis is usually defined by having both dipole components $B_1 = A_1 = 0$ in a quadrupole. With $d \cdot R_{\text{ref}}$ being the distance from the rotation axis to the measuring frame, the two sets of multipoles are related by

$$z_m = z_c - d \cdot R_{\text{ref}} \,, \tag{38}$$

$$C_{m,n} = \sum_{k=n}^{\infty} \frac{(k-1)!}{(n-1)!(k-n)!} C_{c,k} \cdot d^{k-n} \,. \tag{39}$$

This so-called ‘feed-down’ correction is used when the rotation axis cannot be accurately aligned in the magnet, for instance with a magnet aperture small compared to the length. These magnets are measured with ‘moles’ travelling along the aperture [16] or coil shafts with intermediate bearings resting in the magnet [17]. It must be stressed, however, that displacing the reference frame corresponds to describing the field outside the measurement circle, thus extrapolating the measurements outside their validity range. This feed-down correction loses validity for large values of d.

Equation (39) can be simplified, assuming that the coil rotation axis is near the magnet axis, i.e., $d \ll 1$:

$$C_{m,n} = C_{c,n} + n \cdot C_{c,n+1} \cdot d \,. \tag{40}$$

The position of the rotation axis of the measuring system with respect to the the axis of a quadrupole is therefore

$$(d_x + i \cdot d_y) \cdot R_{\text{ref}} = \frac{C_{m,1}}{C_{m,2}} \cdot R_{\text{ref}} \,. \tag{41}$$

Measuring this distance with an accuracy of 0.01 mm is easily achieved for short length measuring coils. As in Section 8.3.1 the issue is to refer the rotation axis to the magnet fiducials. An easy calibration is done when the magnet can be turned upside down.

8.4 Possible configurations according to the magnet size

Figure 18 shows a rotating coil bench measuring linac permanent quadrupoles that are short and small. The motor, the bearings of the rotating coil, and the angular encoder are accurately aligned in a straight line with reference to the base plate.

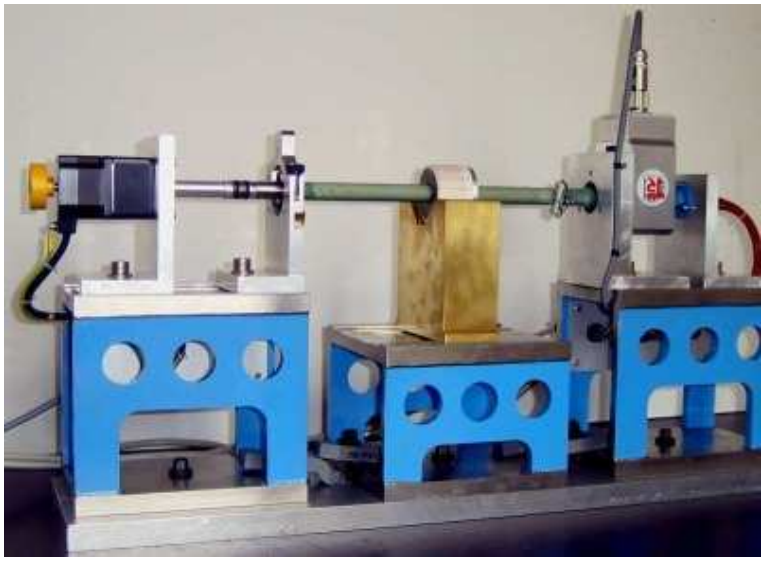

Fig. 18: Bench measuring a small permanent quadrupole magnet for the drift tube of a linac. The motor is on the left and the encoder on the right.

Figure 17 shows in comparison a 15 m long, 35 tonne LHC superconducting dipole magnet. Reference [18] describes the mathematical model established on the series measurement of the LHC superconducting magnets, giving an idea of the size of the measurement project. The measuring shaft [17] in the right part is composed of 12 segments 1.15 m long and separated by ceramic bearings resting on the anti-cryostat, therefore rotating off-axis by up to 3 mm with respect to the symmetry axis of the magnet. By construction, the measuring segments are not accurately aligned azimuthally with respect to each other. Equations (37)–(39) have therefore to be applied to express the results of the measurements in the reference frame of the magnet axis.

Similarly, these LHC magnets were measured by 'moles' [16] in the manufacturing industries. These moles group in one device the coil, motor, and encoder and travel along the magnet length pulled by a cable. Measuring the field direction with the help of an on board inclinometer requires dedicated calibration. Note that other techniques (Section 5, [19]) can measure the magnetic axis of quadrupole magnets.

Figure 19(a) shows a coil structure designed for easy alignment of the magnet with respect to the bearings of the measurement system [20]. This coil setup allows one to separately align the magnetic axis on both magnet ends, then to fine tune the alignment with the full length coil. The full length coil gives the magnet strength, or integrated field, value directly relevant for the accelerator beam. The magnet effective length is obtained by calculating the central field given by the difference between the full length coil and the sum of the end coils. The measurement from the end coils can be compared to 3D simulation of the magnet ends. Note that a measurement with a coil shorter than the magnet is valid only if the longitudinal component of the field is zero on both ends of these coils [14].

Small-aperture magnets render difficult the manufacture of rotating shafts with the coils on both sides of the axis. The solution of Fig. 19(b) is preferred even though the sum of three (or more) data sets must be done. The effective length of the blind parts between the segments must be accurately measured and located where the field does not vary along the axis.

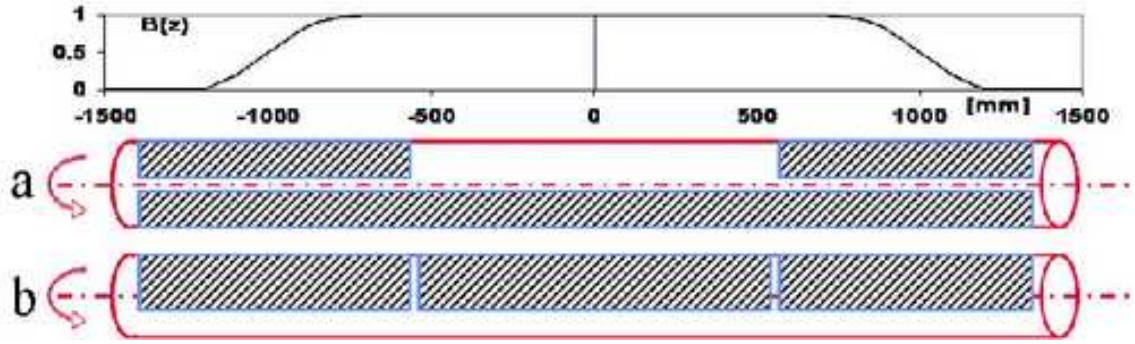

Fig. 19: (a) Coil shaft with a full length coil and two end coils. (b) Separated coil structure when solution (a) cannot be manufactured. It implies blind spaces between the coils.

9 Accuracy limitations of the harmonic coil method

Mechanical or electronic imperfections mainly degrade the measurement of the 'higher order' multipoles, i.e., those with harmonic numbers higher than the magnet multipole order. The three main error sources will be studied in detail:

- voltage integrator offset coupled with irregular rotation rate of the coil,
- error in the coil angle measurement due either to the angular encoder or to torsions of the coil shaft during rotation,
- instability or movement of the rotation axis of the coil shaft due to gravity, bearings quality, or vibrations.

Schemes of compensation coil arrays, connected in opposition, have been developed [21] to remove the signal coming from the magnet main multipole thus allowing the increase of the amplification factor at the input of the integrator. More importantly, these compensation coil assemblies remove non-linear coupling coming from the main harmonic and degrading the high-order harmonic measurement.

9.1 Offset of the integrator coupled with varying rotation rate

Stability of the rotation rate of the harmonic coil does not appear at first order in the method. The angular fluxes, given in Eqs. (8.1)–(33) are explicitly independent of time. However, the voltage integrator has an offset that gives a flux error inversely proportional to the rotation rate. The average offset over a turn can be eliminated afterward by one of the following methods in the case where the field is static during the coil rotation. Obviously, a careful adjustment to zero the voltage offset before the measurement is the most reliable method.

- The coil shaft can continuously rotate if the signal goes via slip rings from the coil to the integrator. The flux integrated over a full turn must be zero if the field is static. This formula is also valid if the current variation is constant and the angle zero corresponds to a zero flux in the coil, but this correction is sensitive to noise in the signal and could be detrimental. The incremental offset can be eliminated at first order by dividing the offset integrated over one turn by the number of angular intervals:
$$\oint \text{Offset} = [\Psi(2\pi) - \Psi(0)_{\text{measured}}] \, . \tag{42}$$
- Without the use of slip rings, the rotating coil has to come back in reverse rotation due to the instrumentation cable. Averaging the incremental fluxes measured during the forward and backward turns removes at first order the offset. Note that it implies as well either a constant or constantly changing current.

Variation of the rotation rate can further be eliminated if the time duration of the individual angular steps are accumulated together with the incremental fluxes and the corresponding correction is applied before the Fourier analysis takes place. Experience has shown that the resulting signal-to-noise enhancement is limited by imperfect removal of this effect, even for rotation rates measured constant within a few per cent.

We will see in Sections 9.3 and 9.5 that most of these degradations of the high order multipole measurement due to electronics can be reduced by the use of compensation coil schemes.

9.2 Measurement errors related to the angle and encoder

The accuracy in measuring the harmonic coefficients of the field depends directly on the angular precision of the integrator triggers. The encoder quality, the torsion of the frame holding the coil or linking it to the encoder must all be considered. Reference [14] gives the formalism to calculate these effects taking into account all kinds of torsions and vibrations. The case of a periodic error when measuring a pure dipole magnet will be detailed here. General equations can be found in Ref. [22].

An angular misalignment between the axis of the encoder and the axis of the coil can lead to a difference between the measured and real angular position of the coil. This error is best approximated by a sine function. A torque on the bearing of the encoder due to a parallel misalignment between these axes gives a similar error of amplitude defined as ϵ:

$$\theta_{\text{meas}} = \theta + \epsilon \cdot \sin\theta \; . \tag{43}$$

A perfect dipole aligned with respect to the measuring equipment is defined by $B_1 = 1$, all other coefficients $B_n, A_n = 0$. As the angular encoder errors are supposed to be small, a first-order estimation gives

$$\Psi(\theta) \propto \cos(\theta_{\text{meas}}) \;\; = \;\; \cos(\theta + \epsilon \cdot \sin\theta) \;\; = \;\; \cos(\theta) - \frac{\epsilon}{2} \cdot (1 - \cos 2\theta) \; . \tag{44}$$

An erroneous quadrupole term, not present in the magnet, will show itself in the Fourier analysis of the integrated voltage. Figure 20 represents it. Its value is related to the amplitude of the error of the encoder by

$$\delta B_2 / B_1 \;\; = \;\; \delta b_2 \;\; = \;\; \frac{\epsilon}{2} \cdot \frac{K_1}{K_2} \; . \tag{45}$$

In order to give orders of magnitude, Eq. (45) can be further simplified with the following hypothesis for the radii sketched in Fig. 15:

$$R_1 = 0 \; , \quad R_2 = R_{\text{ref}} \; .$$

The erroneous quadrupole $\delta b_2 = 10^{-3}$, i.e., 10 units for an angular error $\epsilon = 1$ mrad since the ratio of the sensitivity factors is

$$\frac{K_n}{K_1} = \frac{1}{n} \cdot \left(\frac{R_2}{R_{\text{ref}}} \right)^{n-1} = \frac{1}{n} \; . \tag{46}$$

More generally, any systematic angular error can be decomposed in a Fourier series:

$$\theta_{\text{meas}} = \theta + \sum_k \gamma_k \cos k\theta + \epsilon_k \sin k\theta \; . \tag{47}$$

These γ_k and ϵ_k will generate erroneous normal and skew multipoles when measuring a pure dipole magnet:

$$\begin{aligned} \delta b_n &= \frac{n K_n}{2 K_1} (\epsilon_{n-1} + \epsilon_{n+1}) \; , \\ \delta a_n &= \frac{n K_n}{2 K_1} (\gamma_{n-1} + \gamma_{n+1}) \; . \end{aligned} \tag{48}$$

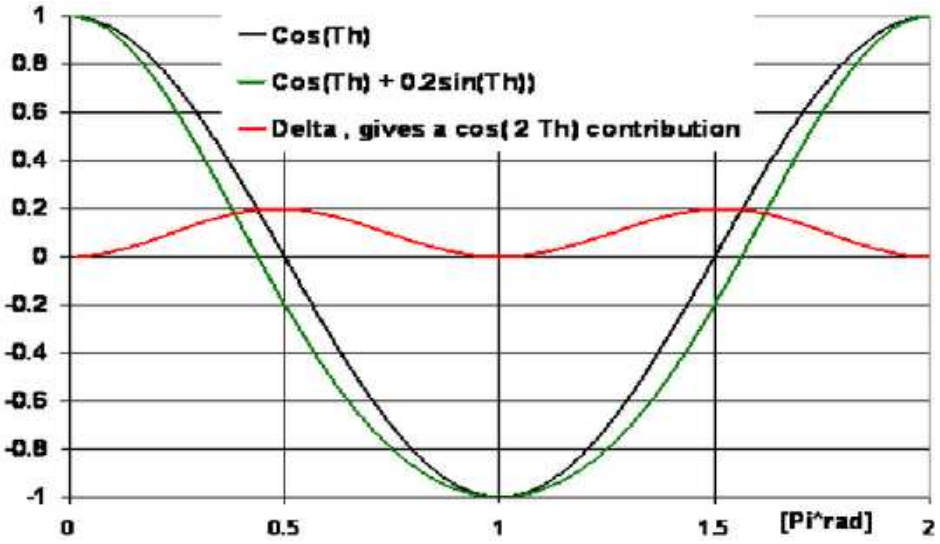

Fig. 20: Flux measured in a dipole with a perfect angle measurement and a first-order error. Their difference gives an erroneous quadrupole term.

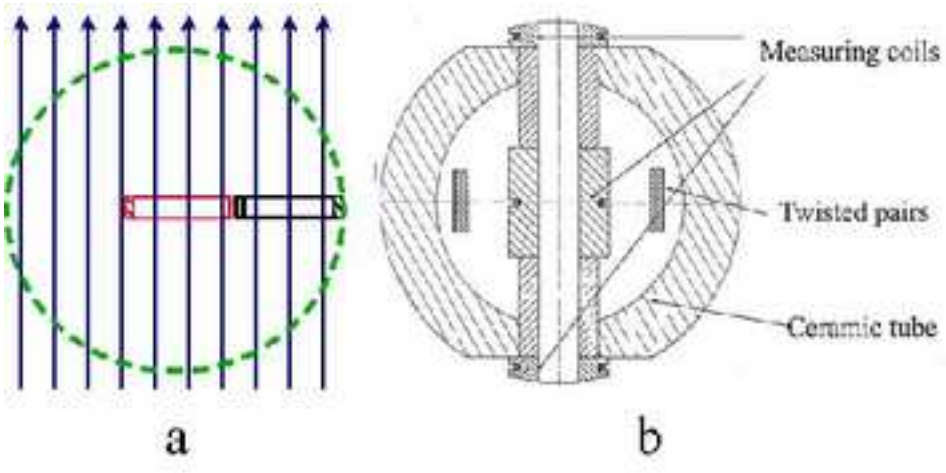

Fig. 21: (a) Assembly of two radial coils with same effective surface connected in opposition to remove the main dipole component from the signal. (b) Cross-section of the three tangential coils as used in Ref. [18]. One of the external coils is kept as a spare.

9.3 Removal of the main harmonic in a dipole magnet by using compensation coil scheme

The previous section shows that high precision in the measurement of the multipoles requires high quality encoders. In addition, the geometry of the equipment to be built, namely the ratio between magnet aperture and length, can lead to severe difficulties in achieving a torsion-free frame holding the coils.

A suitable geometry for the measuring-coil system may be chosen that reduces the angular precision needed. Two coils having the same sensitivity with respect to the dipole term (the same surface) are electrically connected in opposition at the input of the integrator. The resulting sensitivity factor as calculated in Eq. (34) becomes $K_1 = 0$. Their radial positions are sketched in Fig. 21. Consequently, the dipole harmonic is rejected in the flux measured. Rejection ratios of 300 to 2000 can be achieved by sorting the coils according to their effective area and by adjusting them to be parallel. This assembly of coils is sometimes called ‘bucking coils’ in the literature.

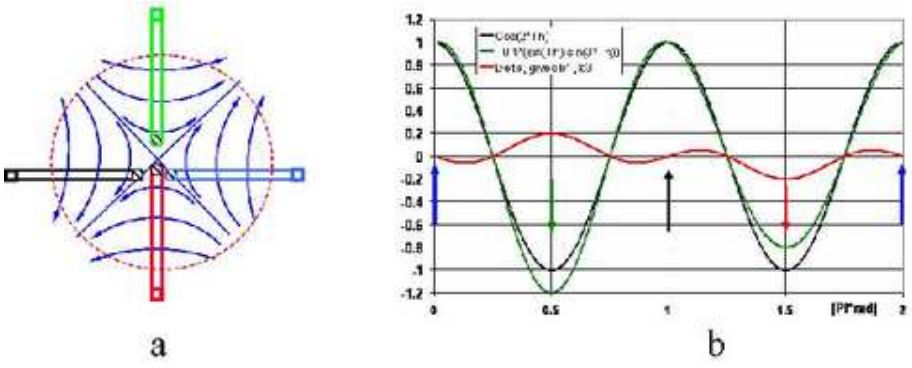

Fig. 22: (a) A non-rigid coil shaft moving up and down, due to gravity, during rotation in a quadrupole field. (b) The flux measured with a perfect rotation and a first-order error. Their difference gives erroneous dipole and sextupole terms.

9.4 Measurement errors related to coil transverse movement

In a dipole magnet, the measuring coil assemblies of Fig. 21, displaced laterally or vertically, will induce no voltage on the integrator connected to it. This is not true if higher harmonics are present or when a quadrupole or sextupole magnet has to be measured. A spurious signal therefore shows up if the mechanics is such that the harmonic coil does not describe a perfect circle when rotating. Calculations show that without proper rejection of the main harmonic, one cannot measure with high accuracy the field quality of a quadrupole.

The deflection of the frame holding the coil gives a simple measure of this effect. The hypothesis is made that the coil is wound on a flat plate that bends due to its own weight when horizontal, and is straight when vertical [Fig. 22(a)]. The centre of the coil consequently moves up and down twice per turn. This vertical displacement of amplitude $d \cdot R_{\text{ref}}$ is approximated by

$$\text{Displ.} = i \cdot d \cdot R_{\text{ref}} \cdot \cos(2\theta) \; . \tag{49}$$

The bounds of the integral of Eq. (31) become with the hypothesis of a simple coil [given by Eq. (46)]

$$\begin{aligned} R_2(\theta) &= R_{\text{ref}} \cdot (i \cdot d \cdot \cos(2\theta) + e^{i\theta}) \; , \\ R_1(\theta) &= R_{\text{ref}} \cdot i \cdot d \cdot \cos(2\theta) \; . \end{aligned} \tag{50}$$

These lateral movements during coil rotation induce non-linear coupling with the quadrupolar field and generate erroneous multipoles of lower and higher orders. Figure 22(b) sketches the curves giving the angular flux with and without this vertical movement. A first-order calculation, i.e., neglecting terms in d^2, into a pure quadrupolar field (only $B_2 \neq 0$) gives the following erroneous skew components:

$$\delta B_1 / B_2 = \delta b_1 = d \tag{51}$$

$$\delta b_3 = -3d \; . \tag{52}$$

A deflection due to gravity of 0.02 mm with $R_{\text{ref}} = 20$ mm (i.e., $d = 0.001$) generates an erroneous dipole corresponding to 0.02 mm of axis displacement and a relative sextupole $b_3 = 0.003$ (or 30 units). This simple calculation therefore stresses the importance of designing a measuring shaft to hold the rotating coils as rigidly as possible, and having as smooth as possible rotation with the help of high-quality bearings and motorisation.

The formal development of the erroneous components created by any transverse movement in any real magnet can be found in Refs. [14]–[22].

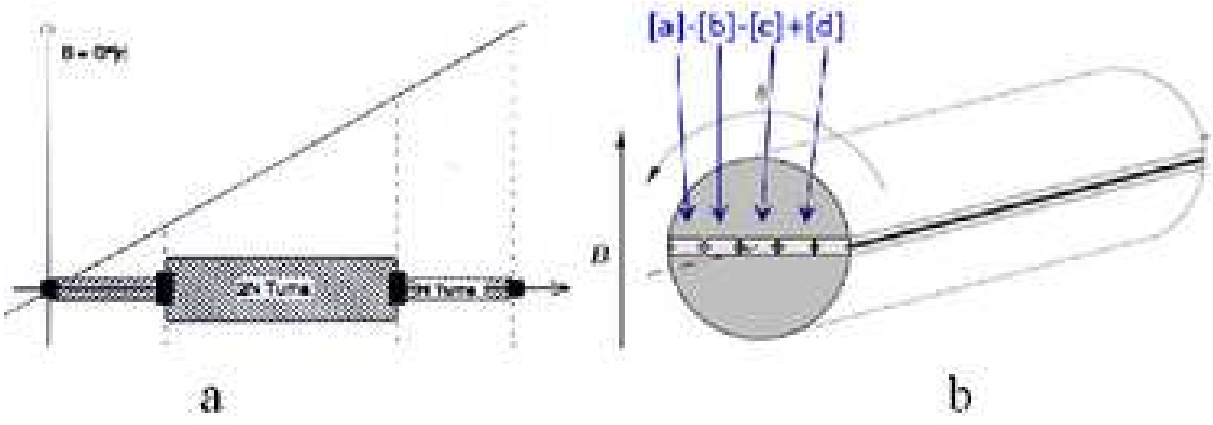

Fig. 23: Two geometries to compensate the dipole and quadrupole components: (a) two coils having the same effective surface, (b) four equal radial coils give the same compensation, one of the external coils is kept as a spare.

9.5 Removal of the main harmonic in a quadrupole magnet by using compensation coil scheme

A coil scheme for an effective removal of the main quadrupole harmonic has to be insensitive to both angular and transverse movements in a pure quadrupole, i.e., to both the quadrupole and dipole sensitivity factors as defined in Eq. (34):

$$K_1 = K_2 = 0\ . \tag{53}$$

The two schemes of Fig. 23 fulfil these two conditions.

It is difficult to have exactly the same effective area for the two coils of the scheme of Fig. 23(a), i.e., the inside coil having half the width and twice the number of turns of the outside one. This scheme induces in addition a high loss of sensitivity to measure the low order multipoles, in particular the sextupole. Although such a coil assembly rejects correctly the quadrupole harmonic, a factor of more than five is lost in sensitivity to measure the sextupole term compared to the sensitivity given by the single external coil. Since this coil assembly is insensitive to any lateral displacement in a quadrupole, turning about another axis will maintain the rejection. A maximum value for the sextupole sensitivity factor K_3 is obtained with the radii of the external coil being [23]:

$$\begin{aligned} R_2 &= R_{\text{ref}}, \\ R_1 &= -1/2 \cdot R_{\text{ref}}\ . \end{aligned} \tag{54}$$

The other scheme is based on four equal coils giving the same geometrical properties [Fig. 23(b) and Fig. 24]. A rejection ratio of more than 100 can be achieved by sorting and careful positioning of the four coil assemblies. Note that these two types of coil assemblies can be used to measure dipole magnets according to Section 9.3 by using only the central and external coils.

10 Calculation of the sensitivity factors of the harmonic coils

10.1 Tangential coil sensitivity

Tangential measuring coils are preferred for easier manufacture and better stability of the rotating coil frame (Section 9.5).

In order to calculate the sensitivity of tangential coils, Eqs. (31)–(34) have to be generalized by putting R_1 and R_2 as 2D variables in the complex plane:

$$K_n = N_t \cdot L \cdot \frac{Z_2^n - Z_1^n}{n \cdot R_r^{n-1}}\ . \tag{55}$$

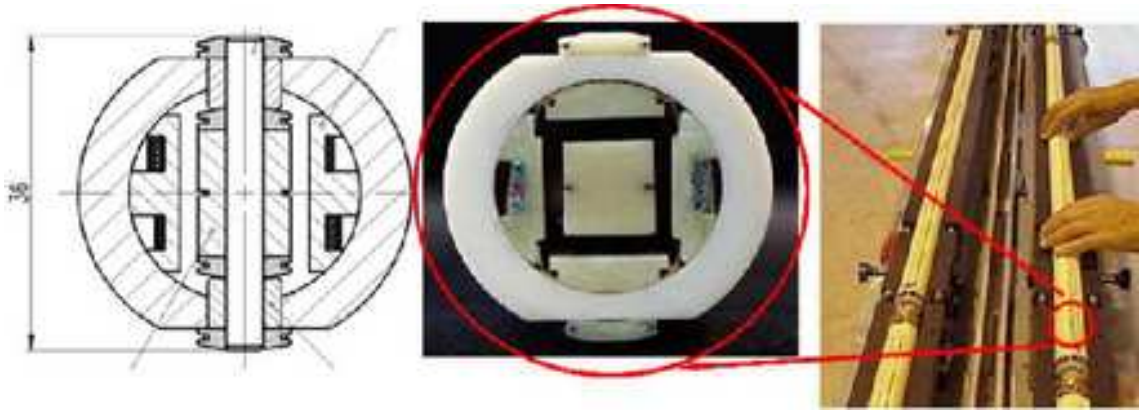

Fig. 24: A compensation coil scheme to measure quadrupoles. Four tangential coils are used to remove the dipole and quadrupole components, one of the external coils is kept as a spare.

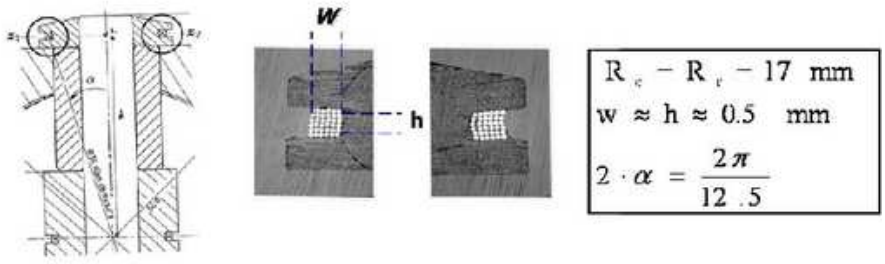

Fig. 25: Parameters of the tangential coil cross-section used for the series measurements of the LHC magnets

The tangential coil of Fig. 25 is horizontal on the y_+ for the first point of rotation and gives real expressions for the K_{2n+1}. The normal components of the multipoles belonging to the dipole symmetry have indeed a vertical field on the y axis. The normal components of the quadrupole, octupole, etc. have an horizontal field on the y axis and the K_{2n} factors have imaginary values. Equation (55) is simplified to

$$K_n = -2 \cdot i^{n+1} \cdot N_t \cdot L \cdot \frac{R_c^n \sin(n\alpha)}{n \cdot R_r^{n-1}} \,, \tag{56}$$

with the two winding positions

$$Z_1 = R_c \cdot e^{i(\pi/2+\alpha)} \,,$$
$$Z_2 = R_c \cdot e^{i(\pi/2-\alpha)} .$$

Equation (56) shows that tangential coils are insensitive to multipole order having an angular period, or an integer number of periods, corresponding to the opening angle. This drawback is easily overcome by having the opening angle either small enough or corresponding to

$$2\alpha = \frac{2\pi}{n+1/2} \,. \tag{57}$$

Note that the K_n would all be imaginary if the tangential coil starts to rotate in vertical position centred on the x_+ axis since the field of all normal components (the B_n) is vertical on the x axis. Equation (55) gives with this hypothesis

$$K_n = -2 \cdot i \cdot N_t \cdot L \cdot \frac{R_c^n \sin(n\alpha)}{n \cdot R_r^{n-1}} \,. \tag{58}$$

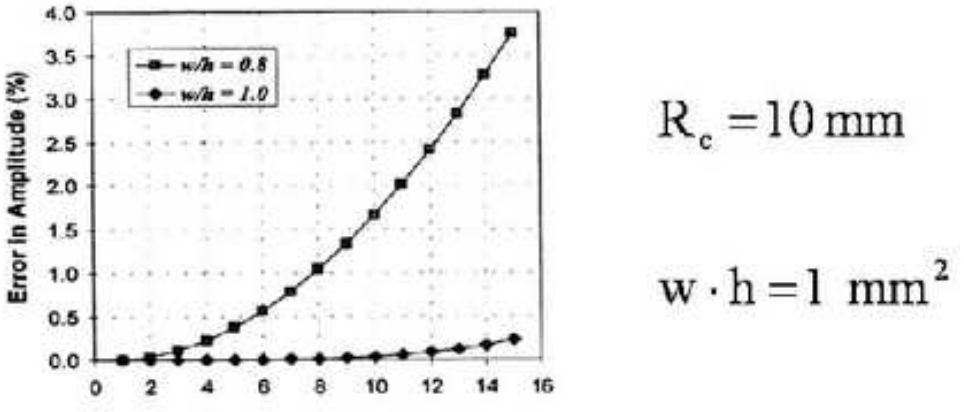

Fig. 26: Error on the sensitivity factor K_n as a function of the multipole order if the winding is considered point-like for a square and rectangular cross-section (courtesy of A. Jain)

Equation (55) is valid for any coil and should be used in the case of compensation coil schemes (Sections 9.3–9.5) where the relative angle between the different coils should be taken into account. General expressions for any ill-positioned coil can be found in Ref. [24].

10.2 The coil winding is not point-like

Equations (34) and (55) are valid for coils having point-like windings. The windings are usually multi-turn and their dimensions, width and height in Fig. 25, should be taken into account by summing the contribution of the position of each individual turn. This summation can be simplified by a normal integral over the section of the winding with the assumption that the density of the turns is homogeneous over this section. The point-like radius of Eq. (55) has to be replaced by the n-order average over the winding section S [24]:

$$\langle Z^n \rangle = \frac{\int_S z^n \cdot \mathrm{d}z}{S} \,. \tag{59}$$

The importance of the corresponding correction is, however, small. Their difference with the point-like case grows with the multipole order whilst the multipole perturbations they measure generally decrease with the order. In addition, the corrections to apply become negligible for square-shaped windings even for high harmonic numbers. This is demonstrated by Fig. 26 extracted from Ref. [22]. A coil winding of 1 mm^2 located at 10 mm radius and calculated with the point-like approximation would give an error of two per mille for the 30-pole ($n = 15$). These effects should therefore be estimated only for measuring coils with aspect ratios far from a square shape like coils based on printed circuits.

11 Experience with the harmonic coil method

11.1 Precision of the measurement of the main field component

The measurement of the field strength integrated over the magnet length, or of the transfer function defined as this integral divided by the current, is usually insensitive to electronic or mechanical noise sources like the shaft rigidity, smoothness of the rotation, vibrations. However, it depends strongly on the calibration of the coil surface for the dipole measurement and the positioning of the coils in the coil frame for quadrupoles and higher order magnets. Techniques for calibrating the coils are described elsewhere in these proceedings. They can be based on measurements with the single stretched wire technique described in Section 4. Accurate measurements of the gains of the electronics and of the excitation current are obviously key elements. Relative precisions of 10^{-4} are obtained to measure dipole magnet strengths and 3 to 10 times worse for quadrupoles with careful calibrations of all elements [9].

11.2 Measuring the higher-order multipoles

The current stability must be extremely high over the turn duration, in the range of ppm to tens of ppm, in order not to create spurious high-order multipoles if measured with a single coil. It is possible to acquire the current value for each incremental flux and apply a first-order correction but this requires a high bandwidth and high-quality measurement.

Experience indicates that the low-order multipoles are more sensitive to the equipment imperfections analysed: voltage integrator offset, rigidity of the frame, irregularities in the rotation giving both torsional and lateral movements. In other words, the sextupole is the difficult multipole to measure in a quadrupole, and that justifies a careful design of the compensation coil scheme to increase K_3 as explained in Section 9.5. Repeatability of 0.01 unit (or 1 ppm relative to the main component) has been achieved in the best cases [25].

The use of compensation schemes improves the measurement of higher-order multipoles for the following reasons.

- The measured signal has a smaller amplitude and can therefore be amplified, reducing electronic noise. It also reduces the errors coming from the offset and the non-linear coupling between offset, rotation rate variations, and signal of the main order harmonic.
- Excitation current variations, including the ripple from the magnet power supply, also couple with the main order signal which is removed with compensation coils. For the same reason, measurements with slowly ramping currents are improved.
- An improvement proportional to the rejection ratio is obtained for all noises generated by mechanical instabilities: displacement of the rotation axis of the coil shaft due to gravity, quality of the bearings, or vibrations.

11.3 Measurement of pulsed magnets with harmonic coils

Measurement of pulsed magnets, i.e., excitation current changing with time, is hardly covered by the rotating coil method. The measurement of the magnet strength, i.e., the main multipole, is spoiled by the field change over the duration of the coil revolution. Accurate synchronization for the measurement of the excitation current at each angular position could be mandatory to get enough precision. Obviously, increasing the rotation rate of the coil shaft and the bandwidth of the electronics greatly helps and must be taken into account at the design phase of the rotating coils, i.e., the highest number of turns for the coil windings is not necessarily the optimum. As an example, the 15 m long coil shaft of Fig. 17 currently measures, at 8 turns per second, the field quality of the LHC magnets with high temporal accuracy.

The measurement of the field quality, i.e., the higher-order multipoles, is greatly improved [26] in this case by the help of a coil scheme to compensate the main multipole (Sections 9.3 and 9.5).

For fast ramping magnets, it is possible to measure flux variation between zero and nominal current with the harmonic coil fixed at a sufficiently large number of angular positions to perform the Fourier analysis. Experimental work is going on at GSI [27] for the FAIR project and at CERN for the new Linac quadrupole magnets having a duty cycle of a few milliseconds. This method requires an accurate angle positioning, obtained for instance by a high-resolution stepping motor. It would bring the advantages of the Morgan coil [3] technique with a simplified coil frame to be manufactured.

12 Conclusion: compare the different measurement techniques

Coils and stretched wires are tools particularly adapted to measurement of accelerator magnets. They give reduced values for parameters controlling particle beams: cross-section components of the field integrated along the magnet length.

The SSW based system can be considered reference equipment to measure in a static field dipole and quadrupole strength, i.e., main field components, where precisions of 10^{-3} to 10^{-4} are needed.

These instruments measure with high accuracy the main field direction and magnetic axis of quadrupole and sextupole magnets. They are being used more and more for these measurement goals in particular with the requirement to better align magnets for synchrotron light sources and with the need for smaller and smaller apertures for high-energy physics accelerators.

Flip coils are a reduced technique of the harmonic rotating coil method. The theory associated with their use is, however, mandatory to correctly measure fast pulsed and curved magnets.

The rotating coil method is a general and accurate method to measure the field quality of magnets: integrated field value, higher order multipoles, and magnetic axis. Recent instrumentation and acquisition systems allow high bandwidth and fully automated measurements. This method is the obvious choice for normal quadrupole magnets, and for superconducting magnets having circular apertures and where beam optics considerations require unprecedented precision in the field quality.

These various methods complement each other. They are complemented by the use of Hall plates for local measurements and of NMR based instruments for high absolute accuracy and calibration. A cross-check between these various methods should be used whenever possible to ascertain precision in magnet measurements.

Acknowledgements

The sections related to the single stretched wire are mostly extracted from the experimental and theoretical work done in different laboratories, in particular by J. Dimarco, A. Jain, A. Temnykh, and Z. Wolf. The list of names of my numerous CERN colleagues who are at the basis of my competence in the field of magnetic measurements is too long to mention here.

References

[1] W. F. Brown and J. H. Sweer, Rev. Sci. Instrum.**16** (1992) 276.

[2] M. I. Green, Search coils, CAS – Measurement and Alignment of Accelerator and Detector Magnets, Anacapri, Italy, 1997, CERN 98-05, p. 143.

[3] G. H. Morgan, Proc. 4th Int. Conf. on Magnet Technology, Upton, NY, 1972, USAEC CONF-720908 (Atomic Energy Commission, Washington, DC, 1973?), p. 787.

[4] A. Jain et al., Field quality measurements at high ramp rates in a prototype dipole for the Fair project, IEEE Trans. Appl. Supercond., vol 18-2, p. 1629, June 2008.

[5] S. Rossi, Developments in proton and light-ion therapy, Proc. EPAC 2006, Edinburgh, 2006 (Jacow, Geneva, 2006), p. 3631.
`http://accelconf.web.cern.ch/AccelConf/e06/PAPERS/FRYAPA01.PDF`.

[6] J. DiMarco et al., Field alignment of quadrupole magnets for the LHC interaction regions, IEEE Trans. Appl. Supercond., vol. 10-1, p. 127, March 2000.

[7] G. Rakowsky et al., Measurement and optimisation of the Visa undulator, Proc. PAC 1999, New York, 1999, (IEEE, Piscataway, 1999),
`http://accelconf.web.cern.ch/AccelConf/p99/PAPERS/THA35.PDF`.

[8] T. C. Fan, C. S. Hwang, and C. H. Chang, A systematic study on the pulsed wire system for magnetic field measurements on the long undulator with high field, Rev. Sci. Instrum. **73** (2002) 1430.

[9] N. Smirnov et al., Focusing strength measurements of the main quadrupoles for the LHC, IEEE Trans. Appl. Supercond., vol. 16-2, p. 261, June 2006.

[10] A. Temnykh, Vibrating wire field-mesuring technique, Nucl. Instrum. Methods Phys. Res., **A 399** (1999) 185.

[11] Z. Wolf, Vibrating wire technique for quadrupole fiducialization, Proc. of 14th International Magnet Measurement Workshop, Geneva, September 2005, http://indico.cern.ch/contributionListDisplay.py?confId=0517

[12] A. Jain, Results from vibrating wire R.D. for alignment of multipoles in NSLS-II, Proc. of 16th International Magnet Measurement Workshop, Bad Zurzach, October 2009, http://immw16.web.psi.ch/Presentations

[13] J. Cobb and D. Horelick, Proc. 3rd Int. Conf. on Magnet Technology, Hambourg, 1970 (DESY, Hambourg, 1972), p. 1439.

[14] W. G. Davies, Nucl. Instrum. Methods, **A311** (1992) 399.

[15] M. Buzio, Fabrication and calibration of search coils, these proceedings.

[16] J. García Pérez et al., Performance of the room temperature systems for magnetic field measurements of the LHC superconducting magnets, IEEE Trans. Appl. Supercond., vol. 16-2, p. 269, 2006.

[17] J. Billan et al., Twin rotating coils for cold magnetic measurements of 15 m long LHC dipoles, IEEE Trans. Appl. Supercond., vol. 10-1, p. 1422, March 2000.

[18] S. Sanfilippo et al., Magnetic performance of the main superconducting magnets for the LHC, IEEE Trans. Appl. Supercond., vol. 18-2, p. 132, 2008.

[19] M. Buzio et al., A device to measure magnetic and mechanical axis of superconducting magnets for the Large Hadron Collider, IEEE Instrumentation and Measurement Technology Conf., Sorrento, Italy, 2006 (IEEE, New York, 2006), p. 759.

[20] O. Pagano, P. Rohmig, L. Walckiers, and C. Wyss, Proc. 8th Int. Conf. on Magnet Technology, Journal de Physique, vol. 45, Colloque C1 (1984), p. 949.

[21] R. M. Main, J. T. Tanabe, and K. Halbach, Measurements and correction of the PEP interaction region quadrupole magnets, IEEE Trans. Nucl. Sci., vol. NS26-3, p. 4030, June 1979.

[22] A. Jain, Harmonic coils, CAS – Measurement and Alignment of Accelerator and Detector Magnets, Anacapri, Italy, 1997, CERN 98-05, p. 175.

[23] L. Walckiers, The harmonic coil method, CAS – Magnetic Measurement and Alignment, Montreux, Switzerland, 1992, CERN 92-05, p. 138.

[24] L. Deniau, Coils calibration, correction factors for rectangular windings, https://edms.cern.ch/file/356512/1/mta-in-98-026.pdf

[25] L. Walckiers et al., Sensitivity and accuracy of the systems for the magnetic measurements of the LHC magnets at CERN, Proc. EPAC 2000, Vienna, Austria (EPS, Geneva, 2000), http://accelconf.web.cern.ch/AccelConf/e00/PAPERS/THP2A17.pdf

[26] J. Buckley, D. Richter, L. Walckiers, and R. Wolf, Dynamic magnetic measurements of superconducting magnets for the LHC, IEEE Trans. Appl. Supercond., vol. 5-2, p. 1024, 1995.

[27] P. Schnizer et al., A mole for measuring pulsed superconducting magnets, IEEE Trans. Appl. Supercond., vol 18-2, p. 1648, June 2008.